

Microbial symbionts buffer host-plants from the demographic costs of environmental stochasticity

Joshua C. Fowler^{a,b,1}, Shaun M. Ziegler^c, Kenneth D. Whitney^c, Jennifer A. Rudgers^c, and Tom E.X. Miller^a

This manuscript was compiled on July 31, 2023

limit = 223 out of 250 words Species' persistence in increasingly variable future climates will depend on resilience against environmental stochasticity, which tends to reduce fitness in fluctuating environments. Most organisms host microbiota that shield against stressful conditions, but deciphering how microbial symbioses buffer against the fitness costs of stochasticity requires experiments encompassing long-term environmental fluctuations. Using cool-season grasses and *Epichloë* fungal endophytes as a model system, we conducted a 14-year symbiont-removal experiment with seven host species and used experimental data to parameterize stochastic demographic models that predict the mean and variance of host fitness. We show that fungal endophytes reduce variance in the fitness of their grass hosts by 10% on average across species and that reductions of up to *In the text you say max variance reduction is 170%. As you know, I don't really like percentages because they are easy to fudge. occur for some hosts. Hosts with "fast" life history traits that lack longevity as an intrinsic buffer experienced the greatest benefits. Under the current climate regime, contributions to host-symbiont mutualism from variance buffering were modest compared to symbiont benefits to mean fitness. However, simulations of increased environmental stochasticity amplified the benefits of variance buffering, which surpassed symbionts' mean effects that have dominated most prior research. These results establish microbial-mediated variance buffering as an important yet cryptic mechanism of resilience to increasing stochasticity under global change.

stochasticity | microbial symbiosis | demography | mutualism

Global climate change involves increases in environmental variability, including changes to precipitation patterns and the frequency of extreme weather events (1, 2). Yet, the ecological consequences of increased variability are less well understood than those of changing climate means, such as long-term warming or drying. Incorporating environmental variability into forecasts of population dynamics can improve predictions of the future.

Classic theory predicts that long-term population growth rates (equivalently, population mean fitness) will decline under increased environmental stochasticity because the costs of bad years outweigh the benefits of good years – a consequence of nonlinear averaging (3, 4). For example, in unstructured populations, the long-term stochastic growth rate in a fluctuating environment (λ_s) will always be lower than the average growth rate ($\bar{\lambda}$) by an amount proportional to the environmental variance (σ^2):

$$\log(\lambda_s) \approx \log(\bar{\lambda}) - \frac{\sigma^2}{2\bar{\lambda}} \quad [1]$$

Populations structured by size or stage similarly experience costs of variability (5, 6). There are accordingly two pathways to increase population viability in a variable environment: increase the mean growth rate and/or dampen temporal fluctuation in growth rates, also called "variance buffering".

Both the characteristics of species and the properties of their environment can buffer demographic fluctuations, including life history traits such as longevity (7, 8), correlations among vital rates (9), transient shifts in population structure (10), the magnitude of environmental variability (11), or the degree of environmental autocorrelation (12, 13). These factors determine the risks of extinction faced by populations (14) and underlie management strategies promoting ecosystem resilience (15). Yet little is known about how biotic interactions influence demographic variability or contribute to variance buffering (16).

Most multicellular organisms host symbiotic microbes that affect growth and performance (17, 18), and many of these are transmitted via reproduction from maternal

Significance Statement

limit = 116 out of 120 words
Many symbiotic microbes benefit hosts under environmental stress, which is becoming more frequent in an increasingly variable climate. Using long-term field experiments with a plant-fungal endophyte model system, we show that, by limiting host exposure to environmental extremes, microbial symbionts reduce their hosts' demographic variance. Because such variance has negative fitness consequences, our results identify variance buffering a novel pathway of host-symbiont mutualism. Species with faster life histories were more strongly buffered by symbiosis, suggesting that microbial symbionts can compensate for the lack of intrinsic tolerance of variability conferred by "slow" life history traits. Increasing stochasticity magnifies the benefits of variance buffering, highlighting a key role of microbial symbionts in promoting host resilience to climate change.

Author affiliations: ^aDepartment of BioSciences, Rice University, Houston, TX, 77005; ^bDepartment of Biology, University of Miami, Miami, FL, 33146; ^cDepartment of Biology, University of New Mexico, Albuquerque, NM, 87131

J.C.F. contributed to data collection, data analysis, and led manuscript drafting. S.Z. contributed to data collection and manuscript revisions. K.D.W. contributed to research conception, data collection, and manuscript revisions. J.A.R. established transplant plots, contributed to research conception, data collection, and manuscript revisions. T.E.X.M. contributed to research conception, data collection, data analysis, and manuscript revisions.

The authors declare no conflict of interest

¹To whom correspondence should be addressed. E-mail: jcf221@miami.edu

hosts to offspring (19). This process of vertical transmission links the fitness of hosts and symbionts in a feedback loop that selects for mutual benefits (20). Many vertically-transmitted microbes are mutualistic and protect hosts from stressful environmental conditions including drought, extreme temperatures, or natural enemies (21, 22). Some of the best studied examples include bacterial symbionts of aphids and other insects that provide their hosts with thermal tolerance through the production of heat-shock proteins (23), and plant-fungal symbionts that produce anti-herbivore toxins (24–26). However, these diverse protective symbioses are context-dependent: the magnitude of benefits depends on environmental conditions (27) and thus will vary temporally in a stochastic environment (28). We hypothesized that context-dependent benefits from symbionts may buffer hosts against variability through strong benefits during harsh periods and neutral or even costly outcomes during benign periods, reducing the impacts of host exposure to extremes and dampening inter-annual variance relative to non-symbiotic hosts. Variance buffering is a previously unexplored mechanism by which symbionts may benefit their hosts instead of or in addition to elevating average fitness, the focus of most previous research.

We tested the hypothesis that context-dependent benefits of symbiosis buffer hosts from the fitness costs of environmental stochasticity. We used cool-season grasses and *Epichloë* fungal endophytes as a tractable experimental model in which non-symbiotic plants can be derived from naturally symbiotic plants through heat treatment, providing a contrast of symbiont effects that controls for the confounding influence of host genetic background. *Epichloë* endophytes are specialized symbionts growing intercellularly in the aboveground tissue of ~30% of cool-season (C_3) grass species (29). These fungi are primarily transmitted vertically from maternal plants through seeds (30). They produce a variety of alkaloids that can protect host plants from herbivory (31) and drought stress (32).

Over 14 years (2007–2021), we collected annual demographic data on the survival, growth, reproduction, and recruitment of all plants within replicated endophyte-symbiotic and endophyte-free populations at our southern Indiana field site. Through taxonomic replication (seven host-symbiont species pairs) we aimed to understand whether host life history traits could explain inter-specific variation in the magnitude of demographic buffering through symbiosis. We used the long-term demographic data to parameterize stochastic population projection models in a hierarchical Bayesian framework. Specifically, we (i) quantified the effects of symbiosis on the mean and variance of host vital rates (survival, growth and reproduction) and fitness, (ii) investigated the relationship between host life history traits and the magnitude of symbiont-mediated variance buffering, (iii) evaluated the relative contribution of mean and variance effects to the overall fitness benefits of symbiosis, and (iv) projected the consequences of symbiont-mediated variance buffering under increased environmental variability.

181
182
183
184
185
186

Results and Discussion

[†]Our experiment began in 2007 with seven grass species that host *Epichloë* fungal endophytes. Located in south-central Indiana, USA, the experiment consisted of annually censused populations founded with either naturally symbiotic plants (S+) or those that had their symbionts experimentally removed via a heat treatment (S-) (See Materials and Methods for a full list of species and experimental methods). The unique data from this long-term experiment are distinctly suitable for detecting fitness benefits of microbial symbiosis that arise through variance buffering, which on average had 13.3 individuals/m² over the course of the experiment. Each census year was a sample of inter-annual climatic variation (n = 14 years; comprising 13 demographic transition years). We fit hierarchical Bayesian generalized linear mixed models to the vital rate data using RStan (33), which allowed us to isolate endophyte effects on vital rate means and variances, borrow strength across species for some variance components, and propagate uncertainty from the individual-level vital rates to population projection models (34). The projection models were stochastic matrix population models parameterized for each host species from the vital rate regressions to quantify endophyte effects on stochastic population growth rates (λ_s) and decompose the overall effect of the symbiosis into contributions through mean vital rates, variance in vital rates, and their interaction (Methods section describes the statistical methods in full).

Quantifying symbiont mediated variance buffering. Across seven host species, eight vital rates, 14 years, and 16,789 individual plants, our analysis provides the first empirical evidence of symbiont-mediated variance buffering. Endophytes reduced inter-annual variance for 66% (37/56) of host species-vital rate combinations (average Cohen's D for effects on vital rate standard deviation: -0.15) (Fig. 1A). Endophytes also increased mean vital rates for the majority (36/56) of host species-vital rate combos (average Cohen's D for effects on vital rate mean: 0.15), and benefits were particularly strong for host survival, plant growth and germination (Fig. 1A). The relative magnitude of symbiont effects on means versus variances differed among host species and their vital rates. For example, endophytes modestly increased mean adult survival (Fig. 1C) and reduced variance in survival (Fig. 1D) for *Festuca subverticillata*, while for *Poa alsodes*, variance buffering was more apparent in seedling growth and inflorescence production (Fig 1E). Interestingly, certain vital rates showed costs of endophyte symbiosis. Symbiotic individuals of *A. perennans* grew larger than those without endophytes (Fig. 1B), yet endophytes also reduced this species' mean germination rates (Fig. 1A). Similarly, endophyte symbiosis increased variance in seedling growth for *Elymus villosus* and *Festuca subverticillata* (Fig. 1A).

Because not all vital rates contribute equally to fitness, we used stochastic matrix models to integrate the diverse effects on vital rates described above into comprehensive measures for the mean and variance of year-to-year fitness (λ_t) and the long-run fitness that integrates both mean and variance (λ_S). On average across host species, endophyte-symbiotic populations had greater mean fitness (> 92% confidence that

[†]I would remove this paragraph here. I've moved some overview elements to the end of the Intro and other bits can be moved to the methods. I think you should get straight into results.

187
188
189
190
191
192
193
194
195
196
197
198
199
200
201
202
203
204
205
206
207
208
209
210
211
212
213
214
215
216
217
218
219
220
221
222
223
224
225
226
227
228
229
230
231
232
233
234
235
236
237
238
239
240
241
242
243
244
245
246
247
248

249 endophytes increased $\bar{\lambda}$) and lower inter-annual variability
250 in fitness (> 86% confidence that endophytes decreased the
251 coefficient of variation of λ_t) than endophyte-free populations
252 (Fig. 2). For some host species, the CV of λ_t was reduced
253 by as much as 170% (*P. alsodes*, *F. subverticillata*), while
254 for others, endophyte effects on variance were substantially
255 smaller (6% lower for *E. villosus*, 16% lower for *A. perennans*),
256 or even positive (27% increase for *E. virginicus*). When
257 mean and variance effects of symbionts were considered
258 together, none of the host-symbiont pairings were antagonistic
259 (i.e., with endophytes that both decreased mean fitness and
260 increased variance) (Fig. 2C), suggesting that variation across
261 host species and vital rates in mean and variance effects may
262 reflect alternative strategies that yield similar benefits of
263 endophyte symbiosis.

264 Reduced sensitivity to drought, as has been reported for
265 some *Epichloë* symbioses (32), is a candidate mechanism that
266 could generate a signature of variance buffering. Accordingly,
267 analysis of climate-explicit matrix models indicated that
268 for five of seven taxa, symbiotic populations were less
269 sensitive to annual or growing season drought (12-month
270 or 3- month drought index; Standardized Precipitation-
271 Evapotranspiration Index (35)) than symbiont-free popula-
272 tions (Supporting Information Text; Fig. S24-S25; Table S3).
273 However, we did not find a strong relationship between the
274 magnitude of variance buffering and relative drought sensitivities,
275 suggesting that other climatic factors or other temporally-
276 varying aspects of the environment may elicit benefits of
277 endophyte symbiosis, including documented resistance to
278 herbivory for six host taxa (36, 37). Identifying the potentially
279 complex relationships between vital rates and environmental
280 drivers remains a key challenge for accurate forecasts of the
281 ecological impacts of environmental stochasticity (38).[†]

282 **Life history analysis.** Long-lived species, those on the slow
283 end of the slow-fast life history continuum, are expected to
284 be less sensitive to environmental variability (39), a pattern
285 which has empirical support across plants (40) and animals
286 (8, 41). Therefore, we predicted that host species with long
287 lifespans that produce few, large offspring would benefit less
288 from the variance buffering effects of endophytes than species
289 with fast life cycles that produce many smaller offspring with
290 low per-capita chance of success (42, 43). In support of this
291 prediction, symbionts with trait values representing faster
292 life history strategies experienced greater variance buffering
293 from endophytes than those with slow life histories (Fig. 3).
294 Bayesian phylogenetic mixed-effects models, controlling for
295 species' relatedness, indicated that variance buffering was
296 stronger for host species with shorter lifespan (Fig. 3A; 75%
297 probability of positive relationship with empirically observed
298 max age) and smaller seeds (Fig. 3B; 73% probability of
299 positive relationship with seed length). Other life history
300 traits similarly had positive but weaker support for the
301 prediction that faster life history traits would correlate with
302 stronger variance buffering (Fig. S26-S28). Additionally, the
303 three host species for which the overall mutualism was weakest
304 (*Elymus villosus*, *Elymus virginicus*, and *Poa sylvestris*)
305 (Fig. 2C) were the only hosts for which we observed fungal
306 stromata, fruiting bodies capable of horizontal (contagious)
307 transmission (Table S2), in line with theoretical expectations

311 for strict vertical transmission driving the evolution of strong
312 host-symbiont mutualisms (20, 44). Conclusions about life
313 histories are somewhat constrained by the narrow range of
314 trait values among these closely related species in the grass
315 sub-family Pooideae. Our understanding of how life history
316 variation modulates the fitness consequences of microbial
317 symbiosis would profit from tests across a wider span of
318 taxonomic groups (45).

319 **Relative contributions of mean and variance effects.** To
320 evaluate the relative importance of mean fitness benefits
321 and variance buffering as alternative pathways of mutualism,
322 we decomposed the overall effect of the symbiosis on the
323 stochastic growth rate λ_s using simulations of four versions
324 of population models that included both mean and variance
325 buffering effects, mean effects alone, variance effects alone, or
326 neither mean nor variance effects. Overall, the full effect of
327 symbiosis on λ_s , averaged across host species, provided strong
328 evidence of grass-endophyte mutualism (100% certainty of a
329 positive total effect on λ_s) (Fig. 4; see Fig. S21 for individual
330 host species).[§] Contributions to this total effect derived
331 from both mean and variance buffering effects, as well as
332 a slightly negative interaction (i.e., the combined influence
333 of mean and variance effects was lower than the sum of
334 their individual effects). Endophytes' contributions to λ_s
335 from mean effects were four times greater, averaged across
336 species, than contributions from variance buffering (Fig. 4),
337 suggesting that, under the regime of environmental variability
338 represented by our 14-year study, damped fluctuation in
339 fitness is a far less important element of the benefits of
340 symbiosis than elevated mean fitness.

341 **Consequences of variance buffering under increased envi-
342 ronmental variability.** Simulations of increased environmental
343 variability, a key prediction of climate change forecasts (2),
344 indicated that mutualism with microbial symbionts, and their
345 variance buffering effects in particular, will take on increased
346 importance for grasses in a more variable future climate. To
347 simulate increased variability, we repeated the decomposition
348 of λ_s under two additional scenarios, randomly sampling
349 transition matrices from either the six or two most extreme
350 years experienced by each species, subsets of the thirteen
351 transition matrices across the study period. The six- and
352 two-years scenarios increased the standard deviation of yearly
353 growth rates by 1.3 and 2.1 times, respectively, without
354 changing mean growth rates (< 2.3% difference in $\bar{\lambda}$ between
355 simulation treatments)(See SM; Fig. S21-22). Increased
356 variability elicited stronger mutualistic benefits of endophyte
357 symbiosis (Fig. 3) than ambient variability (overall effect
358 of the symbiosis increased by > 130%). This increase was
359 driven by increased contributions from the variance buffering
360 mechanism (from a 24% contribution in the ambient scenario
361 to a 66% contribution in the most variable scenario). In the
362 most variable scenario, the relative importance of mean and
363 variance effects reverses, with variance buffering contributions
364 that are 1.5 times greater than contributions from mean
365 benefits, averaged across species (Fig. 4). Thus, variance
366 buffering – a cryptic microbial influence that manifests over
367 long temporal scales – is poised to become the dominant

368
369
370
371
372
[†]It would be nice if we could briefly summarize here our certainty in the total effect by species.
e.g. All host species experience positive effects on λ_s through endophyte symbiosis and our
statistical certainty of host-symbiont mutualism ranged from XX to XX%. Or something like that.

way in which grasses benefit from symbiosis with fungal endophytes in more variable future climates.

Ecologists increasingly recognize the importance of symbiotic microbes for host organisms and the populations, communities, and ecosystems in which their hosts reside (46–49). Despite awareness of these ubiquitous interactions, long-term studies of microbial symbiosis are very rare. Our analysis of taxonomically-replicated, long-term field experiments manipulating the presence/absence of fungal symbionts in plants demonstrates for the first time that heritable microbes can commonly benefit hosts not only through improved mean fitness – the focus of most previous research – but also via buffering against environmental variance. Our results provide an important advance to improve forecasts of the responses of populations (and symbiota) to increasing environmental stochasticity under global change, suggesting that, for some host species, microbial symbiosis may compensate for the lack of intrinsic tolerance of variability conferred by “slow” life history traits. We found that symbiont-mediated variance buffering made relatively weak contributions to host-symbiont mutualism under the current regime of environmental variability, but is likely to become the dominant benefit that fungal endophytes confer to grass hosts in more variable future environments. This result emerges from the context-dependent nature of grass-endophyte interactions, combined with the observation that environmental stochasticity generates fluctuation in context. These key ingredients, and thus the potential for symbiont-mediated variance buffering, similarly apply to the diverse host-microbe symbioses across the tree of life.

Materials and Methods

Study site and species. This study was conducted at Indiana University’s Lilly-Dickey Woods Research and Teaching Preserve (39.238533, -86.218150) in Brown County, Indiana, USA. This site is part of the Eastern broadleaf forests of southern Indiana, where the ranges of many understory cool-season grass species overlap. The experiment focused on seven of these grasses which host *Epichloë* endophytes (*Agrostis perennans*, *Elymus villosus*, *Elymus virginicus*, *Festuca subverticillata*, *Lolium arundinaceum*, *Poa alsodes*, and *Poa sylvestris*) (Table S1).

Endophyte removal, plant propagation, and field set-up. Seeds from naturally symbiotic populations of the seven focal host species were collected during summer-fall 2006 from Lilly-Dickey Woods and the nearby Bayles Road Teaching and Research Preserve (39.220167, -86.542683). To generate symbiotic (S+) and symbiont-free (S-) plants from the same genetic lineages, seeds from each species were disinfected with a heat treatment described in Table S1 or left untreated. [¶] The heat treatment created symbiont-free plants by warming seeds to temperatures at which the fungus becomes inviable but the host seeds can still germinate. Both heat-treated and untreated seeds were surface sterilized with bleach to remove epiphyllous microbes, cold stratified for up to 4 weeks, then germinated in a growth chamber before transfer to the greenhouse at Indiana University where they grew for ~8 weeks. We confirmed endophyte status by staining thin sections of inner leaf sheath with aniline blue and examining tissue for fungal hyphae at 200X magnification (50). We established experimental populations with vegetatively propagated clones of similar sizes. By starting the experiment with plants of similar sizes and the same number of unique genotypes, we aimed to limit any potential effects of heat treatments on initial plant growth (51).

[¶]In the main text you did not really use S+ and S- after defining this, so I cut it. Do the same here if you don't consistently use it in the methods.

During the fall of 2007 and spring of 2008, we established 10 3x3 m. plots for *A. perennans*, *E. villosus*, *E. virginicus*, *F. subverticillata*, and *L. arundinaceum* and 18 plots for *P. alsodes* and *P. sylvestris*. Half of the plots were randomly assigned to be planted with either symbiotic or with symbiont-free plants, and initiated with 20 evenly spaced individuals labeled with aluminum tags. In spring 2008, we placed plastic deer net fencing around each plot to limit deer herbivory and disturbance; damaged fences were regularly replaced.

Long-term demographic data collection. Each summer starting in 2008 through 2021, we censused all individuals in each plot for survival, growth and reproduction, adding new recruits to the census. We censused each species during its peak fruiting stage (May: *Poa alsodes*, *Poa sylvestris*; June: *Festuca subverticillata*; July: *Elymus villosus*, *Elymus virginicus*, *Lolium arundinaceum*; September: *Agrostis perennans*), such that the censuses were pre-breeding and new recruits came from the previous years’ seed production. Leaf litter was cleared out of each plot prior to the census, to aid in locating plants. For each plant remaining from the previous year, we determined survival, measured its size as a count of tillers, and collected reproductive data as counts of reproductive tillers and seed-bearing spikelets on all reproductive tillers to a maximum of three. We also tagged all unmarked individuals that were recruits from the previous years’ seed production and collected the same demographic data. New recruits typically had one tiller and were non-reproductive. In 2008 and 2009, we took additional counts of seeds per inflorescence for all reproducing individuals in the plots to ground-truth our sub-sample estimates. For *Agrostis perennans*, we also collected seed counts in 2010. In 2018, we stopped collecting data for the *Lolium arundinaceum* plots, which had very high survival and low recruitment, and consequently very low variation across years. For each individual in the experiment, our data record their transitions in size and reproduction from one year to the next. In total across 14 years, the dataset includes demographic information for 16,789 individual host-plants and 31,216 transition-year observations.

We expected plots to maintain their endophyte status (S+ or S-) because the fungal symbionts are almost exclusively vertically transmitted, and plots were spaced a minimum of 5 m apart, limiting seed dispersal or horizontal transmission of the symbiont between plots. However, we regularly confirmed endophyte treatment throughout the lifetime of the experiment by opportunistically taking subsets of seeds from reproductive individuals and scoring them for their endophyte status with microscopy as above. Overall, these scores reflected 98% faithfulness of recruits to their expected endophyte status across species and plots (Fig. S23; Supplement data). Additionally, we have rarely observed fungal stromata, the fruiting bodies by which *Epichloë* are potentially transmitted horizontally, provided the fly vector is also present (52). For *A. perennans*, *F. subverticillata*, *L. arundinaceum*, and *P. alsodes*, we never observed stromata. We observed stromata only infrequently for *E. villosus*, and even more rarely for *E. virginicus* and *P. sylvestris* (Table S2). For these species, stromata have only been observed on 35, 4, and 6 plants respectively, making up < 0.3% of all censused plants (Supplemental data). These stromata observations occurred irregularly across years; in most years there were no stromata during the census, and in a few years several plants produced stromata.

Vital rate modeling. Equipped with these demographic data, we fit statistical models for survival, growth, flowering (yes or no), fertility of flowering plants (number of flowering tillers), production of seed-bearing spikelets (number per inflorescence), the average number of seeds per spikelet, and the recruitment of seedlings from the preceding year’s seed production (Fig. S1 - S10). We fit these vital rates as generalized linear mixed models in a hierarchical Bayesian framework using RStan (33). All vital rate models included random plot and year effects, with separate estimates of year-to-year variance for symbiotic and symbiont-free plants, to quantify the effect of endophytes on inter-annual variance (Fig. S11 - S18). These variance components and other predictors as described below were given vague priors (53). We ran each vital rate model for 2500 warm-up and 2500 MCMC sampling iterations with three chains. We assessed model convergence with trace

plots of posterior chains and checked for \hat{R} values less than 1.01, indicating low within- and between-chain variation (54, 55). For those models that showed poor convergence, we extended the MCMC sampling to include 5000 warm-up and 5000 sampling iterations, which was only necessary for seedling growth. We graphically checked vital rate model fit with posterior predictive checks comparing simulated data from 500 posterior draws with the observed data (Fig. S19-S20).

Survival - We modeled survival as a Bernoulli process, where the survival (S) of an individual i in plot p and census year t was predicted by the plot-level endophyte status (e), host species (h), size in the preceding census, and the plant's origin status (whether it was initially transplanted or naturally recruited into the plot).

$$S_{i,p(e),h,t} \sim \text{Bernoulli}(\hat{S}_{i,p(e),h,t}) \quad [2a]$$

$$\text{logit}(\hat{S}_{i,p(e),h,t}) = \beta_{0h} + \beta_1 * \text{origin}_i \quad [2b]$$

$$+ \beta_{2h} * \text{endo}_i + \beta_{3h} * \text{size}_{i,t-1} + \tau_{e,h,t} + \rho_p \quad [2c]$$

$$\tau_{e,h,t} \sim \text{Normal}(0, \sigma_{\tau_{e,h}}^2) \quad [2d]$$

$$\rho_p \sim \text{Normal}(0, \sigma_\rho^2) \quad [2e]$$

Here, \hat{S} is the survival probability ($p(e)$) indicates that plot identity is uniquely associated with an endophyte status), β_{0h} is an intercept specific to each host species, β_1 is the effect of the plant's recruitment origin, β_{2h} is the endophyte effect, β_{3h} is the size effect, $\tau_{e,h,t}$ is a normally distributed year effect for each species and endophyte status with variance $\sigma_{\tau_{e,h}}^2$, and ρ_p is a normally distributed plot effect with variance σ_ρ^2 . We assume that origin effect β_1 and plot-to-plot variance σ_ρ^2 are shared across host species, allowing us to "borrow strength" across the multi-species dataset; other model parameters are unique to host species. We separately modeled the survival of newly recruited seedlings, which were typically one tiller and non-reproductive, with a similar model but omitting size dependence and the effect of the plant's origin status. All random effects were estimated independently between seedling and adult vital rates models.

Growth - We modeled plant size in census year t (G) with the same linear predictor for the mean as described for survival. Because we measured size as positive integer-valued counts of tillers, we modeled it with a zero-truncated Poisson-inverse Gaussian distribution. This distribution includes a shape parameter λ_G to account for overdispersion in the data. We additionally modeled the growth of newly recruited seedlings separately with a Poisson-inverse Gaussian model omitting size structure and the plants' origin status as with seedling survival.

Flowering - We modeled whether or not a plant was flowering during the census (P) as a Bernoulli process, with the same linear predictor for the mean as described above for survival except that size dependence for reproductive vital rates was determined by the individual's size during the same census year as opposed to its size during the previous year.

Fertility - For a plant that was flowering during the census, its fertility was the number of reproductive tillers produced (F), which we modeled as a function of size in the same census period with a zero-truncated Poisson-Inverse Gaussian distribution, with the same linear predictor for the mean as described above.

Spikelets per Inflorescence - Spikelet production (K) was recorded as integer counts on up to three inflorescences per reproducing plant. We modeled these data with a negative binomial distribution, with the same linear predictor for the mean as described above.

Seed Production per Spikelet - For individuals with recorded counts of seed production, we calculated the number of seeds per spikelet from our counts of seeds and spikelets per inflorescence, and then modeled seeds per spikelet (D) as means of a Gaussian distribution for each species and endophyte status. Because we had less detailed data across years and plants for seed production than for other reproductive vital rates, we omitted both plot and year random effects.

Seedling Recruitment - We used a binomial distribution to model the recruitment of new seedlings (R) into the plots from seeds produced in the preceding year, assuming no long-lived seed bank. We included an intercept specific to each host and endophyte

status and the same random effects structure as in other models. We estimated the number of seeds per plot in the preceding year by multiplying the total number of reproductive tillers per plant by the mean number of spikelets per inflorescence on that plant and by a sample from the posterior distribution of mean number of seeds per spikelet (D). For plants with missing fertility or spikelet data, we used the expected number of reproductive tillers (F) or of spikelets per inflorescence from (K), drawing from the full posteriors of our models. We rounded this value to get the estimated seed production for each individual, and finally summed across all reproductive plants in each year and plot to get the total number of seeds produced.

Stochastic population model. Using the fitted vital rate models, we parameterized stochastic matrix projection models including two state variables: r_t (the number of newly recruited individuals in year t), and n_t (a vector including all non-seedling individuals of sizes $x \in \{1, 2, \dots, U\}$, ranging from one to the maximum number of tillers U). We used the same model structure for each species and endophyte status (not shown in model notation, to make it more readable). The total number of recruits in year $t + 1$ is given by:

$$r_{t+1} = \sum_{x=1}^U P(x; \boldsymbol{\tau}_P) F(x; \boldsymbol{\tau}_F) K(x; \boldsymbol{\tau}_K) DR(\boldsymbol{\tau}_R) n_t^x \quad [3]$$

The total number of seeds produced by a maternal plant of size x is the product of the size-specific probability of flowering P , the number of reproductive tillers F , the number of spikelets per inflorescence K , and the number of seeds per spikelet D . Multiplying by the probability of transitioning from seed to seedling R gives a per-capita rate of seedling production, which is multiplied by the number of plants of size x (n_t^x , the x^{th} element of n_t) and summed. Each function also depends on the species- and endophyte-specific year random effects for that vital rate ($\boldsymbol{\tau}$, a vector of year-specific values derived from the statistical models).

Recruitment, survival and growth determine the rest of the population dynamics of the new seedlings and larger plants. The number of y -sized plants in year $t + 1$ is given by:

$$n_{t+1}^y = Z(y; \boldsymbol{\tau}_Z) B(\boldsymbol{\tau}_B) r_t + \sum_{x=1}^U S(x; \boldsymbol{\tau}_S) G(x, y; \boldsymbol{\tau}_G) n_t^x \quad [4]$$

where n_{t+1}^y is the y^{th} element of vector n_{t+1} . The first term on the right hand side of Eqn. 4 represents growth (Z) and survival (B) of seedling recruits. The second term includes the survival of x -sized plants and the growth of survivors from size x to y , summed over all x . To avoid predictions of unrealistic growth outside of the observed size distribution, we set a ceiling on the growth function for plants at the 97.5th percentile in the observed size distribution (56).

Each of the functions in Eqns. 3 and 4 have separate intercepts and year random effects for symbiotic and symbiont-free populations, allowing us to calculate the effect of endophyte symbiosis on the mean and variance of λ , the dominant eigenvalue of the projection matrix. Analysis of climate-explicit population models followed the same logic as for the climate-implicit models presented here with the addition of parameters defining the relationship between either annual or growing season drought index and each vital rate. A full description of climate-explicit methods can be found in the Supporting Information Text.

Life History Analysis. We collected metrics describing each host species' life history to test the relationship between pace of life and variance buffering (Table S1). Using the Rage package (57), we calculated R_0 , longevity, and generation time from our estimated transition matrices using the S- mean matrix as the reference condition. We recorded seed size as the average lemma length from the Flora of North America (58). We also calculated and the 99th percentile of maximum observed age for each species from their S- populations. Next, we fit Bayesian phylogenetic mixed-effects models using the 'brms' package (59) to test the relationship between each life history trait and the estimated effect of symbiosis on the coefficient of variation from the population model while

controlling for phylogenetic non-independence in the hosts (Fig. 26) and the symbiont (Fig. S27). We pruned larger species-level phylogenies of plants(60) and *Epichloë* fungi (61) to include the focal species. *Agrostis perennans* was not included in the tree, and so we used a congeneric species, *A. hyemalis*. We defined separate phylogenetic covariance matrices for each pruned tree. We propagated uncertainty in the estimated variance buffering effect with a measurement error model. Thus the model for the variance buffering effect V was given by:

$$\begin{aligned} V_{MEAN,h} &\sim Normal(V_{EST,h}, V_{SD,h}) & [5a] \\ V_{EST,h} &\sim Normal(\mu_h, \sigma) & [5b] \\ \mu &= \alpha + \beta * trait + \pi & [5c] \\ \alpha &\sim Normal(0, .5) & [5d] \\ \beta &\sim Normal(0, .1) & [5e] \\ \sigma &\sim Half-Normal(.044, .01) & [5f] \\ \pi &\sim Normal(0, \sigma_\pi * \mathbf{A}) & [5g] \\ \sigma_\pi &\sim Half-Normal(0, .1) & [5h] \end{aligned}$$

Here, V_{EST} is the variance buffering effect for each host species h , estimated from the posterior mean (V_{MEAN}) and standard deviation (V_{SD}), propagating uncertainty associated with the effect of symbiosis in our population model. The model includes an intercept parameter (α) and a slope parameter (β) defining the relationship between the variance buffering effect and the life history trait. The residual standard deviation is given by (σ). We used weakly informative priors to aid model convergence. Each prior was centered at zero, except for the residual standard deviation, which we centered at the standard deviation of the estimated variance buffering effect, .04. The phylogenetic random effect (π) has a standard deviation (σ_π) which is structured by the covariance matrix \mathbf{A} . We ran each MCMC sampling chain for 8000 warmup iterations and 2000 sampling iterations. We assessed model convergence as described for the vital rate models.

Mean-variance decomposition. To calculate stochastic population growth rates (λ_s) for each host species and endophyte status we simulated population dynamics for 1000 years by randomly sampling from the 13 annual transition matrices observed over the course of the experiment, discarding the first 100 years to minimize the influence of initial conditions. Sampling observed transition matrices produces models which realistically capture inter-annual variation by preserving correlations between vital rates (62). We tallied the total population size at each time step as $N_t = r_t + \sum_{x=1}^U n_t^x$ and calculated the stochastic growth rate as $\log(\lambda_s) = E[\log(\frac{N_t}{N_{t+1}})]$ (63, 64). We calculated the total effect of endophyte symbiosis as the difference in λ_s between S+ and

S- populations. We propagated uncertainty from the vital rate models to the calculation of λ_s using 500 draws from the posterior distribution of model parameters.

We decomposed the total endophyte effect on λ_s into contributions from effects on vital rate means, variances, and their interaction. Specifically, we repeated the calculation of λ_s for two additional “treatments”: (1) endophyte effects on mean vital rates only, with inter-annual variances shared between S+ and S- at the S- reference level for all vital rates, and (2) endophyte effects on vital rate variances only, with vital rate means shared between S+ and S- at the S- reference level. The combination of all four λ_s treatments (S+ vital rate means and variances, S- means and variances, S+ means with S- variances, S- means with S+ variances) allowed us to quantify to what extent the overall effect of symbiosis derives from changes in vital rates means, variances, and their interaction. The interaction occurs because the variance penalty to stochastic growth is proportional to the mean value of annual growth rates (see Eq. 1) such that variance is more detrimental for populations with low average growth rates. For each contribution element (variance buffering, mean effects, and their interaction), we calculated a cross-species mean to assess the overall contributions (Fig. 4).

Simulation experiment. To create scenarios of increased variance relative to that observed during the study period, we repeated the

stochastic growth rate estimation and decomposition, but sampling only a subset of the 13 observed annual transition matrices. We created two scenarios of increased environmental variance by sampling the transition matrices associated with the six or two most extreme λ values, representing the six or two best and worst years, using S- populations as the reference condition. By sampling away from an average year in both directions, the mean value of annual growth rates remained similar across treatments ($\bar{\lambda}$ averaged across species: All years = 0.71; 6 years = 0.71; 2 years = 0.73; Fig. S21A), while the standard deviation more than doubled ($sd(\lambda)$ averaged across species: All years = 0.25; 6 years = 0.34; 2 years = 0.54 ; Fig. S21B), representing elevated environmental fluctuations. We performed the same mean-variance decomposition for these scenarios as for the ambient conditions (all 13 years sampled) for all host species described above (Fig. S22).

ACKNOWLEDGMENTS. We thank Mark Sheehan, Ali Campbell, Kyle Dickens, Blaise Willis, and Sar Lindner for contributions to field data collection. We also thank Volker Rudolf, Daniel Kowal, Lydia Beaudrot and Judie Bronstein for helpful discussion of this project and manuscript. This research was supported by the National Science Foundation Division of Environmental Biology awards 1754468 and 2208857.

1. S Seneviratne, et al., *Changes in climate extremes and their impacts on the natural physical environment*. (Cambridge University Press), (2012).
2. IPCC, Climate change 2021: The physical science basis (2021).
3. RC Lewontin, D Cohen, On Population Growth in a Randomly Varying Environment. *Proc. Natl. Acad. Sci.* **62**, 1056–1060 (1969) Publisher: National Academy of Sciences Section: Biological Sciences: Zoology.
4. SD Tuljapurkar, Population dynamics in variable environments. III. Evolutionary dynamics of r-selection. *Theor. Popul. Biol.* **21**, 141–165 (1982).
5. JE Cohen, Comparative statics and stochastic dynamics of age-structured populations. *Theor. population biology* **16**, 159–171 (1979).
6. S Tuljapurkar, *Population dynamics in variable environments*. (Springer Science & Business Media) Vol. 85, (2013).
7. CA Pfeifer, Patterns of variance in stage-structured populations: evolutionary predictions and ecological implications. *Proc. Natl. Acad. Sci.* **95**, 213–218 (1998).
8. WF Morris, et al., Longevity can buffer plant and animal populations against changing climatic variability. *Ecology* **89**, 19–25 (2008).
9. A Compagnoni, et al., The effect of demographic correlations on the stochastic population dynamics of perennial plants. *Ecol. Monogr.* **86**, 480–494 (2016).
10. MM Ellis, EE Crone, The role of transient dynamics in stochastic population growth for nine perennial plants. *Ecology* **94**, 1681–1686 (2013).
11. RC Rodríguez-Caro, et al., The limits of demographic buffering in coping with environmental variation. *Oikos* **130**, 1346–1358 (2021).
12. S Tuljapurkar, SH Orzack, Population dynamics in variable environments i. long-run growth rates and extinction. *Theor. Popul. Biol.* **18**, 314–342 (1980).
13. J Fieberg, SP Ellner, Stochastic matrix models for conservation and management: a comparative review of methods. *Ecol. letters* **4**, 244–266 (2001).
14. ES Menges, Applications of population viability analyses in plant conservation. *Ecol. Bull.* **6** —pp. [10.1073/pnas.XXXXXXXXXX](https://doi.org/10.1073/pnas.XXXXXXXXXX)
15. A Kuparinen, A Boit, FS Valdovinos, H Lassaux, ND Martinez, Fishing-induced life-history changes degrade and destabilize harvested ecosystems. *Sci. reports* **6**, 22245 (2016).
16. CH Hilde, et al., The Demographic Buffering Hypothesis: Evidence and Challenges. *Trends Ecol. & Evol.* **0** (2020) Publisher: Elsevier.
25. K Saikkonen, PE Gundel, M Helander, Chemical ecology mediated by fungal endophytes in grasses. *J. chemical ecology* **39**, 962–968 (2013).
26. M Neyaz, DR Gardner, R Creamer, D Cook, Localization of the swainsonine-producing chaetothyriales symbiont in the seed and shoot apical meristem in its host ipomoea carnea. *Microorganisms* **10**, 545 (2022).
27. SA Chamberlain, JL Bronstein, JA Rudgers, How context dependent are species interactions? *Ecol. letters* **17**, 881–890 (2014).
28. P Jordano, Spatial and temporal variation in the avian-frugivore assemblage of prunus mahaleb: patterns and consequences. *Oikos* pp. 479–491 (1994).
29. A Leuchtmann, Systematics, distribution, and host specificity of grass endophytes. *Nat. toxins* **1**, 150–162 (1992).
30. GP Cheplick, S Faeth, SH Faeth, *Ecology and evolution of the grass-endophyte symbiosis*. (OUP USA), (2009).
31. D Brem, A Leuchtmann, Epichloë grass endophytes increase herbivore resistance in the woodland grass brachypodium sylvaticum. *Oecologia* **126**, 522–530 (2001).
32. FA Decunta, LI Pérez, DP Malinowski, MA Molina-Montenegro, PE Gundel, A systematic review on the effects of epichloë fungal endophytes on drought tolerance in cool-season grasses. *Front. plant science* **12**, 644731 (2021).
33. Stan Development Team, RStan: the R interface to Stan (2022) R package version 2.21.7.
34. BD Elderd, TE Miller, Quantifying demographic uncertainty: Bayesian methods for integral projection models. *Ecol. Monogr.* **86**, 125–144 (2016).
35. SM Vicente-Serrano, S Beguería, JL López-Moreno, A multiscalar drought index sensitive to global warming: the standardized precipitation evapotranspiration index. *J. climate* **23**, 1696–1718 (2010).

- 745 36. JA Rudgers, K Clay, An invasive plant-fungal mutualism reduces arthropod diversity. *Ecol. Lett.* **11**, 831–840 (2008). 807
- 746 37. KM Crawford, JM Land, JA Rudgers, Fungal endophytes of native grasses decrease insect 808
747 herbivore preference and performance. *Oecologia* **164**, 431–444 (2010). 809
- 748 38. J Ehrén, WF Morris, Predicting changes in the distribution and abundance of species under 810
749 environmental change. *Ecol. letters* **18**, 303–314 (2015). 811
- 750 39. GI Murphy, Pattern in life history and the environment. *The Am. Nat.* **102**, 391–403 (1968). 812
- 751 40. A Compagnoni, et al., Herbaceous perennial plants with short generation time have 813
752 stronger responses to climate anomalies than those with longer generation time. *Nat. communications* **12**, 1–8 (2021). 814
- 753 41. C Le Coeur, NG Yoccoz, R Salguero-Gómez, Y Vindenes, Life history adaptations to 815
754 fluctuating environments: Combined effects of demographic buffering and lability. *Ecol. Lett.* **25**, 2107–2119 (2022). 816
- 755 42. M Rees, Evolutionary ecology of seed dormancy and seed size. *Philos. Transactions Royal Soc. London. Ser. B: Biol. Sci.* **351**, 1299–1308 (1996). 817
- 756 43. AT Moles, M Westoby, Seedling survival and seed size: a synthesis of the literature. *J. Ecol.* **92**, 372–383 (2004). 818
- 757 44. ME Afkhami, JA Rudgers, Symbiosis lost: imperfect vertical transmission of fungal 819
758 endophytes in grasses. *The Am. Nat.* **172**, 405–416 (2008). 820
- 759 45. JM Jeschke, H Kokko, The roles of body size and phylogeny in fast and slow life histories. 821
760 *Evol. Ecol.* **23**, 867–878 (2009). 822
- 761 46. ME Afkhami, SY Strauss, Native fungal endophytes suppress an exotic dominant and 823
762 increase plant diversity over small and large spatial scales. *Ecology* **97**, 1159–1169 (2016). 824
- 763 47. E Smith, G Vaughan, R Ketchum, D McParland, J Burt, Symbiont community stability 825
764 through severe coral bleaching in a thermally extreme lagoon. *Sci. Reports* **7**, 2428 (2017). 826
- 765 48. JW Dallas, RW Warne, Captivity and animal microbiomes: potential roles of microbiota for 827
766 influencing animal conservation. *Microb. Ecol.* pp. 1–19 (2022). 828
- 767 49. L Wu, et al., Reduction of microbial diversity in grassland soil is driven by long-term climate 829
768 warming. *Nat. Microbiol.* **7**, 1054–1062 (2022). 830
- 769 50. CW Bacon, JF White, Stains, media, and procedures for analyzing endophytes in 831
770 *Biotechnology of endophytic fungi of grasses*. (CRC Press), pp. 47–56 (2018). 832
- 771 51. JA Rudgers, AL Swafford, Benefits of a fungal endophyte in elymus virginicus decline under 833
772 drought stress. *Basic Appl. Ecol.* **10**, 43–51 (2009). 834
- 772 52. TL Bultman, JF White Jr, TI Bowdish, AM Welch, J Johnston, Mutualistic transfer of 835
773 epichloë spores by phorbia flies. *Mycologia* **87**, 182–189 (1995). 836
- 773 53. J Gabry, D Simpson, A Vehtari, M Betancourt, A Gelman, Visualization in bayesian 837
774 workflow. *J. Royal Stat. Soc. Ser. A: Stat. Soc.* **182**, 389–402 (2019). 838
- 774 54. SP Brooks, A Gelman, General methods for monitoring convergence of iterative simulations. 839
775 *J. computational graphical statistics* **7**, 434–455 (1998). 840
- 775 55. A Gelman, J Hill, *Data analysis using regression and multilevel/hierarchical models*. 841
776 (Cambridge university press), (2006). 842
- 776 56. JL Williams, TE Miller, SP Ellner, Avoiding unintentional eviction from integral projection 843
777 models. *Ecology* **93**, 2008–2014 (2012). 844
- 777 57. OR Jones, et al., Rcompadre and rage—two r packages to facilitate the use of the 845
778 compadre and comrade databases and calculation of life-history traits from matrix 846
779 population models. *Methods Ecol. Evol.* **13**, 770–781 (2022). 847
- 779 58. (year?). 848
- 780 59. PC Bürkner, brms: An R package for Bayesian multilevel models using Stan. *J. Stat. Softw.* 849
781 **80**, 1–28 (2017). 850
- 781 60. AE Zanne, et al., Three keys to the radiation of angiosperms into freezing environments. 851
782 *Nature* **506**, 89–92 (2014). 852
- 782 61. A Leuchtmann, CW Bacon, CL Schardl, JF White Jr, M Tadych, Nomenclatural realignment 853
783 of neotyphodium species with genus epichloë. *Mycologia* **106**, 202–215 (2014). 854
- 784 62. CJ Metcalf, et al., Statistical modelling of annual variation for inference on stochastic 855
785 population dynamics using integral projection models. *Methods Ecol. Evol.* **6**, 1007–1017 856
786 (2015). 857
- 786 63. H Caswell, Matrix population models: Construction, analysis, and interpretation. 2nd edn 858
787 sinauer associates. Inc., Sunderland, MA (2001). 859
- 787 64. M Rees, SP Ellner, Integral projection models for populations in temporally varying 860
788 environments. *Ecol. Monogr.* **79**, 575–594 (2009). 861
- 789 851
- 790 852
- 791 853
- 792 854
- 793 855
- 794 856
- 795 857
- 796 858
- 797 859
- 798 860
- 799 861
- 800 862
- 801 863
- 802 864
- 803 865
- 804 866
- 805 867
- 806 868

Figures

869	931
870	932
871	933
872	934
873	935
874	936
875	937
876	938
877	939
878	940
879	941
880	942
881	943
882	944
883	945
884	946
885	947
886	948
887	949
888	950
889	951
890	952
891	953
892	954
893	955
894	956
895	957
896	958
897	959
898	960
899	961
900	962
901	963
902	964
903	965
904	966
905	967
906	968
907	969
908	970
909	971
910	972
911	973
912	974
913	975
914	976
915	977
916	978
917	979
918	980
919	981
920	982
921	983
922	984
923	985
924	986
925	987
926	988
927	989
928	990
929	991
930	992

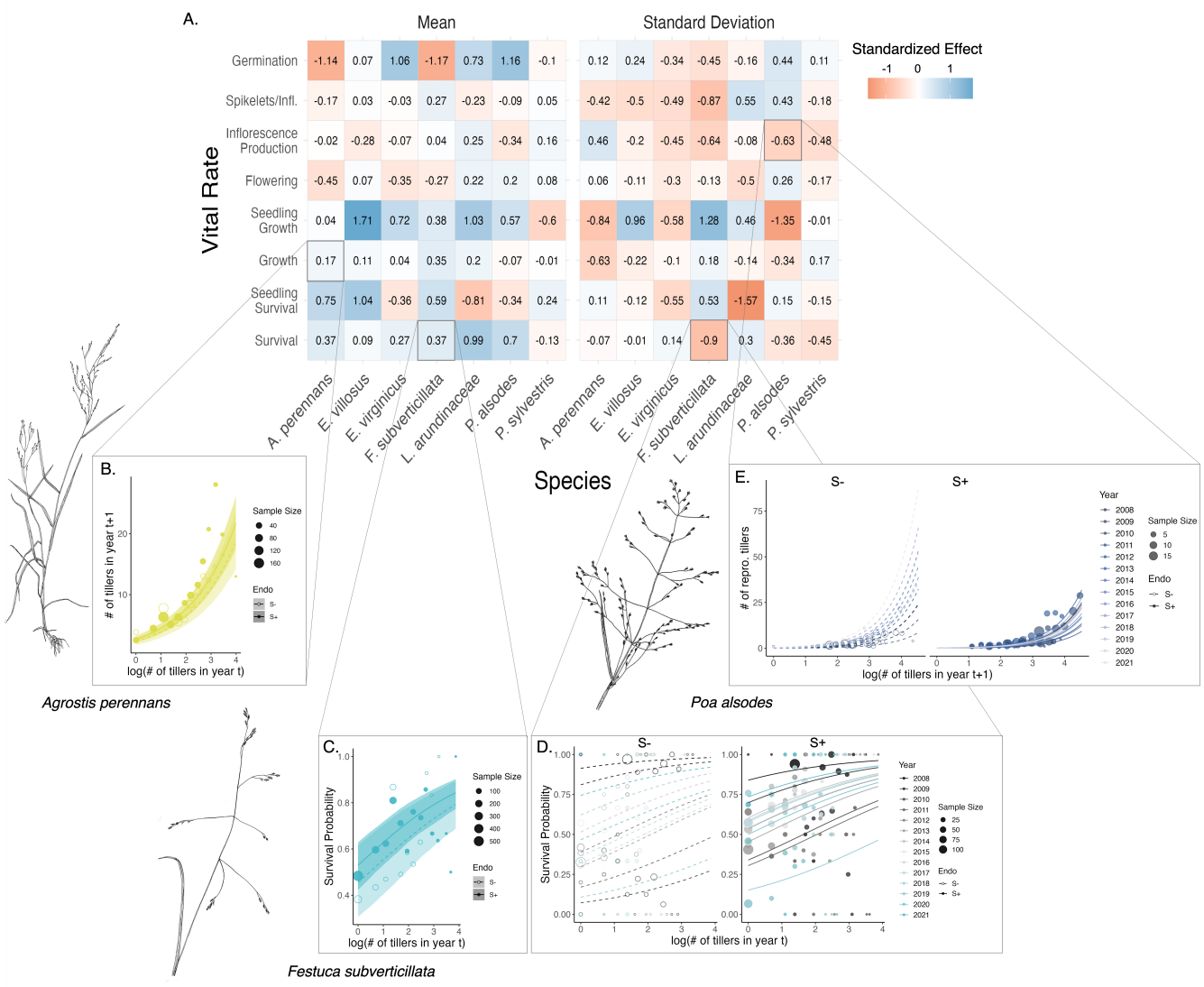


Fig. 1. Endophyte symbiosis altered host vital rates.(A) Shading represents the posterior mean standardized effect size (Cohen's D) of endophyte symbiosis on mean or standard deviation of host vital rates (blue indicates that symbiosis increased the mean or standard deviation and red indicates a reduction). Endophytes' diverse vital rate effects include increased (B) mean growth of *A. perennans* and (C) mean survival probability of *F. subverticillata*. Endophyte presence also reduced inter-annual variance in (D) the survival of *F. subverticillata* and (E) the fertility of *P. alsodes*. Organism silhouettes modified from "Festuca subverticillata" by Cindy Roché and "Agrostis hyemalis" and "Poa alsodes" by Sandy Long ©Utah State University.

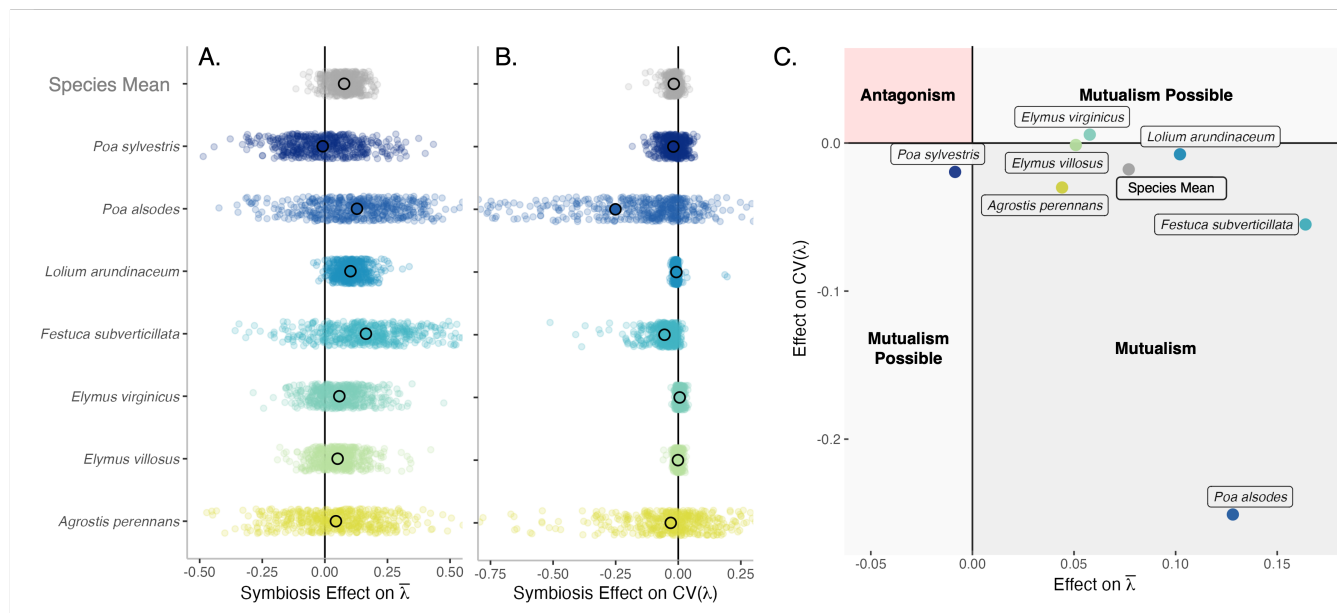


Fig. 2. Mean and variance-buffering effects on fitness. Black circles indicate the average effect of endophytes along with 500 posterior draws (smaller colored circles) on the (A) mean and (B) coefficient of variation in λ for each host species as well as a cross species mean. (C) For all hosts, endophytes either reduce variance, increase the mean, or both, and consequently when considering stochastic environments, the interactions are always at least potentially mutualistic.

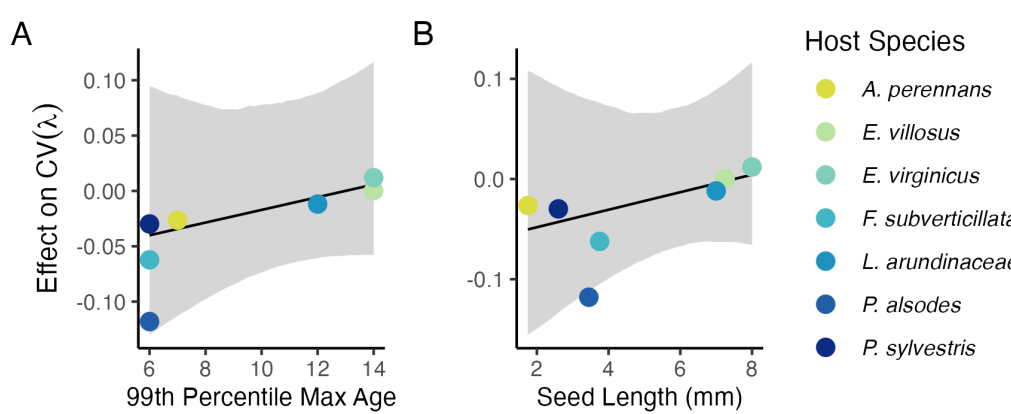


Fig. 3. Host species with faster life history traits experience stronger effects of symbiont-mediated variance buffering. Regressions between life history traits describing the fast-slow life history continuum ((A) 99th percentile maximum age observed during long term censuses in years; (B) Seed size) and the effect of endophyte symbiosis on the coefficient of variation in population growth rate (λ). Each panel shows the fitted mean relationship (line) along with the 95% credible interval.

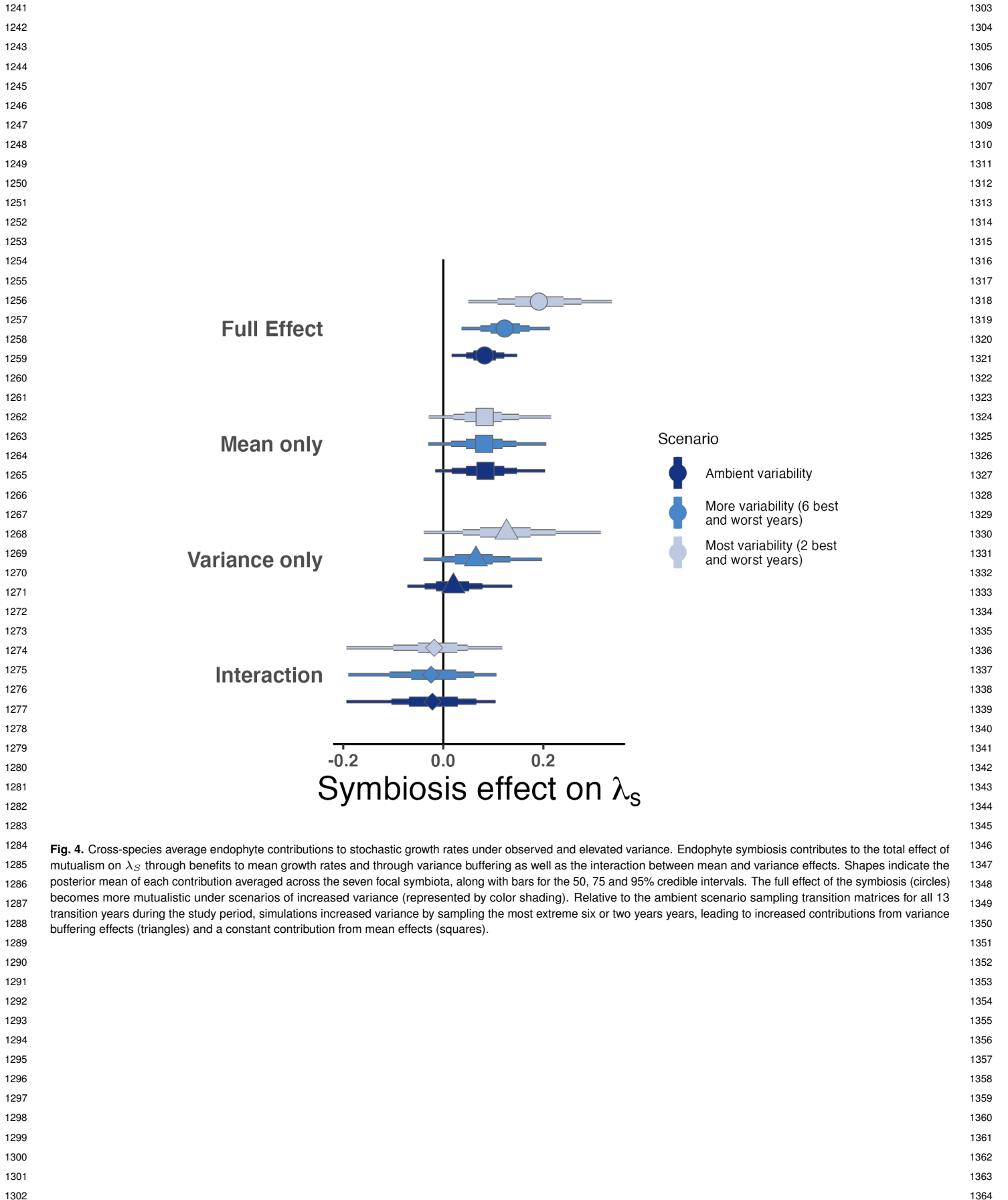


Fig. 4. Cross-species average endophyte contributions to stochastic growth rates under observed and elevated variance. Endophyte symbiosis contributes to the total effect of mutualism on λ_s through benefits to mean growth rates and through variance buffering as well as the interaction between mean and variance effects. Shapes indicate the posterior mean of each contribution averaged across the seven focal symbionts, along with bars for the 50, 75 and 95% credible intervals. The full effect of the symbiosis (circles) becomes more mutualistic under scenarios of increased variance (represented by color shading). Relative to the ambient scenario sampling transition matrices for all 13 transition years during the study period, simulations increased variance by sampling the most extreme six or two years years, leading to increased contributions from variance buffering effects (triangles) and a constant contribution from mean effects (squares).